Sensors and Actuators B 234 (2016) 353–360

Contents lists available at ScienceDirect

Sensors and Actuators B: Chemical

journal homepage: www.elsevier.com/locate/snb

Extremely sensitive ethanol sensor using Pt-doped SnO_2 hollow nanospheres prepared by Kirkendall diffusion

Bo-Young Kim, Jung Sang Cho, Ji-Wook Yoon, Chan Woong Na, Chul-Soon Lee, Jee Hyun Ahn, Yun Chan Kang, Jong-Heun Lee*

Department of Materials Science and Engineering, Korea University, Seoul 136-713, Republic of Korea

ARTICLE INFO

Article history:
Received 3 December 2015
Received in revised form 11 April 2016
Accepted 2 May 2016
Available online 3 May 2016

Keywords:
SnO_2
Gas sensor
Hollow spheres
Kirkendall diffusion
Sensitivity

ABSTRACT

The pure and 0.3 wt% Pt-doped SnO_2 hollow nanospheres were prepared by the oxidation of pure and Pt-doped Sn nanocrystals embedded in carbon matrix and their gas sensing characteristics were investigated. The formation of hollow morphology was attributed to the nanoscale Kirkendall effect due to rapid outward diffusion of Sn ions and relatively slow inward diffusion of oxygen. Pure SnO_2 hollow nanospheres showed a high response (resistance ratio) of 93.3 when exposed to 5 ppm ethanol. The response to 5 ppm ethanol was significantly increased to 1399.9 with doping 0.3 wt% Pt. In addition, selectivity to ethanol was also enhanced by Pt doping. Ultrasensitive and selective detection of ethanol in pure and Pt-doped SnO_2 nanospheres is explained by the effective electron depletion in hollow structures and catalytic promotion of gas sensing reaction.

1. Introduction

Oxide semiconductor gas sensors have irreplaceable advantages such as high gas response, small size, and cost-effectiveness [1]. There have been efforts to enhance the gas response of oxide semiconductors in order to detect trace concentration of harmful, explosive, and toxic gases. The techniques investigated by researchers include, loading with noble metal catalysts, decreasing the particle size, controlling the inter-particle or inter-nanostructure conduction, and incorporating highly gas-accessible porous nanostructures [1–4].

Oxide hollow spheres with thin shells provide an excellent nano-architecture for highly sensitive gas sensors [5,6] because the entire hollow structure with its high gas accessibility can participate in gas sensing reaction. To date, various chemical fabrication routes have been explored to prepare specific oxide semiconductor hollow structures for gas sensors; these include spray pyrolysis [7], template-free hydrothermal/solvothermal self-assembly [8,9], sacrificial template methods [10], layer-by-layer coating [11], microemulsion methods [12], and Ostwald ripening [13].

The Kirkendall diffusion process is another viable chemical route to develop a well-defined hollow morphology during oxidation of metals or metal precursors, and occurs when the outward diffusion of cation is substantially faster than the counter-diffusion of oxygen [14]. Compared to conventional template-based synthesis of hollow spheres of highly crystalline oxides, self-templated solid evacuation via Kirkendall diffusion has the advantages of good scalability, low cost, and simplicity of the synthetic process. In addition, the diameter and shell thickness of the SnO_2 hollow spheres can be controlled by tuning the size and oxidation kinetics of Sn nanocrystals.

NiO nanotubes [15] and CuO hollow spheres [16] prepared by the Kirkendall diffusion process have been explored as gas sensors. However, research on the design of high performance gas sensors using oxide hollow spheres prepared by Kirkendall diffusion is still in the nascent stage. The most representative sensing material, tin oxide, has been prepared in the form of hollow SnO_2 spheres [17] and Sn@void@SnO/SnO_2 yolk-shell spheres [18] by nanoscale Kirkendall diffusion only for application in the electrodes of Li-ion batteries. However, to the knowledge of the authors, investigations into gas sensors using pure and Pt-doped SnO_2 hollow nanospheres prepared by self-templated Kirkendall diffusion have been barely investigated.

In the present contribution, pure and Pt-doped SnO_2 hollow nanospheres were synthesized by spray drying of pure and Pt-doped SnC_2O_4-polyvinylpyrrolidone (PVP) precursors, the formation of Sn-carbon(C) and Pt-doped Sn-C composite spheres by crystallizing Sn component and carbonizing PVP in reducing atmosphere, and subsequent solid evacuation by Kirkendall

* Corresponding author at: Department of Materials Science and Engineering, Korea University, Anam-Dong, Sungbuk-Gu, Seoul 136-713, Republic of Korea.
E-mail address: jongheun@korea.ac.kr (J.-H. Lee).

http://dx.doi.org/10.1016/j.snb.2016.05.002
0925-4005/

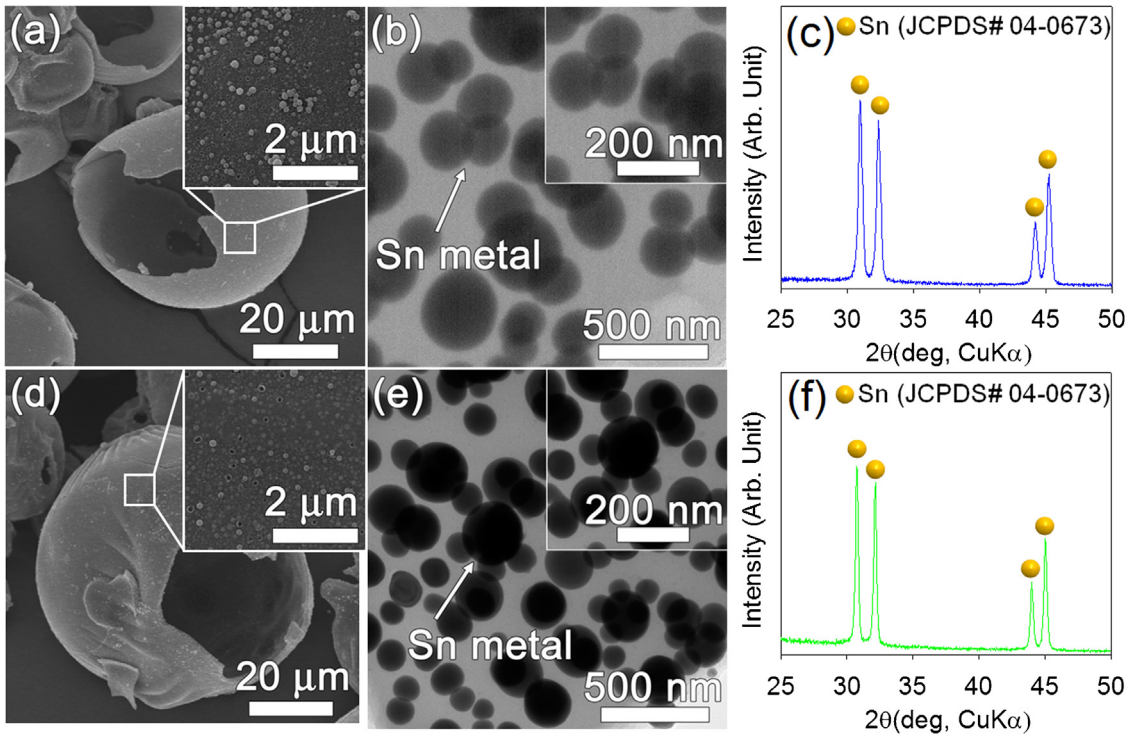

Fig. 1. SEM/TEM images and X-ray diffraction patterns of (a–c) Sn-C and (d–f) Pt-doped Sn-C composite spheres.

diffusion during the oxidation of Sn nanocrystals. The pure SnO_2 hollow nanospheres showed excellent ethanol sensing characteristics, while the Pt-doped SnO_2 hollow nanospheres showed ultrahigh response and selectivity to ppm-level ethanol. The main focus of this study is to understand the relationship between the immense gas response of Pt-doped SnO_2 hollow nanospheres and the hollow morphology and catalytic function of Pt.

2. Experimental

2.1. Sample preparation

Spray drying was used to prepare spherical precursors of the SnO_2 hollow nanospheres. The spray solution for pure SnO_2 nanospheres was prepared by dissolving 21.095 g of tin(II) oxalate (SnC_2O_4, 99.9%, Sigma-Aldrich Co., LLC, USA) and 10 g of polyvinylpyrrolidone (PVP, MW ≤ 1,300,000, Sigma-Aldrich Co., LLC, USA) in 1 L of distilled water. For the preparation of 0.3 wt% Pt-doped SnO_2 hollow spheres, 0.120 g of chloroplatinic acid hexahydrate ($H_2PtCl_6{\cdot}6H_2O$, Sigma-Aldrich Co., LLC, USA) was added to the above spray solution. A two-fluid nozzle was used as an atomizer, and the atomization pressure was fixed at 1.0 bar (100 kPa). The temperatures at the inlet and outlet of the spray dryer were 250 and 120 °C, respectively. The spray-dried pure and Pt-doped SnC_2O_4-PVP composite microspheres were stabilized at 150 °C for 1 h in an air atmosphere. These were then converted into solid carbon spheres with embedded pure and Pt-doped Sn nanocrystals by carbonization of the PVP and crystallization of the Sn precursors through heat treatment at 400 °C in a 10% H_2/Ar atmosphere for 3 h. Subsequent heat treatment of the Sn-C and Pt-doped Sn-C composite spheres at 500 °C in an air atmosphere for 5 h (heating rate: 5 °C min^{-1}) leads to the formation of pure and Pt-doped SnO_2 hollow nanospheres by Kirkendall diffusion during oxidation of the Sn nanocrystals. To investigate the role of hollow morphology on the gas sensing characteristics, commercial SnO_2 nanopowders (Tin(IV) oxide, Sigma-Aldrich Co., LLC., USA) were also used to prepare gas sensors.

2.2. Characterization

The phase and crystallinity of the powders were analyzed by X-ray diffractometry (XRD, D/MAX-2500 V/PC, Rigaku, Japan, Source: CuKα), and the chemical state of each sample was examined by X-ray photoelectron spectroscopy (XPS, MultiLab 2000, Thermo Scientific, USA). Morphologies of the powders were investigated by field emission scanning electron microscopy (FESEM, S-4800, Hitachi Co., Ltd., Japan) and transmission electron microscopy (HR-TEM, Talos F200 X, Hillsboro, OR, USA). The specific surface areas and pore size distributions were determined from a Brunauer–Emmett–Teller (BET) analysis of nitrogen adsorption measurements (TriStar 3000, Micromeritics). The heat-treatment temperature of precursor spheres was determined by thermogravimetric (TG) analysis (Q600, TA Instruments, USA).

2.3. Gas sensing characterization

The pure and 0.3 wt% Pt doped-SnO_2 hollow nanospheres were lightly pulverized and dispersed in distilled water. The slurry was dripped onto an alumina substrate (size: 1.5 mm × 1.5 mm, thickness: 0.25 mm) having two Au electrodes (electrode width: 1 mm, electrode spacing: 0.2 mm) using a micro pipette. The sensor temperatures were controlled using the micro heater and were measured using an IR temperature sensor (Metis MP25, Sensortherm GmBH, Germany). The substrate temperature was controlled between 325 and 450 °C by adjusting the heater powers in the range of 294–485 mW. The sensors were contained in a specially designed, low-volume (1.5 cm^3) quartz tube to minimize any delay in changing their surrounding atmosphere. Before measurement, the sensor was heated to 450 °C for 3 h to remove residual water and to stabilize the sensors. The thicknesses of three sensing films using commercial SnO_2 powders, pure SnO_2 hollow

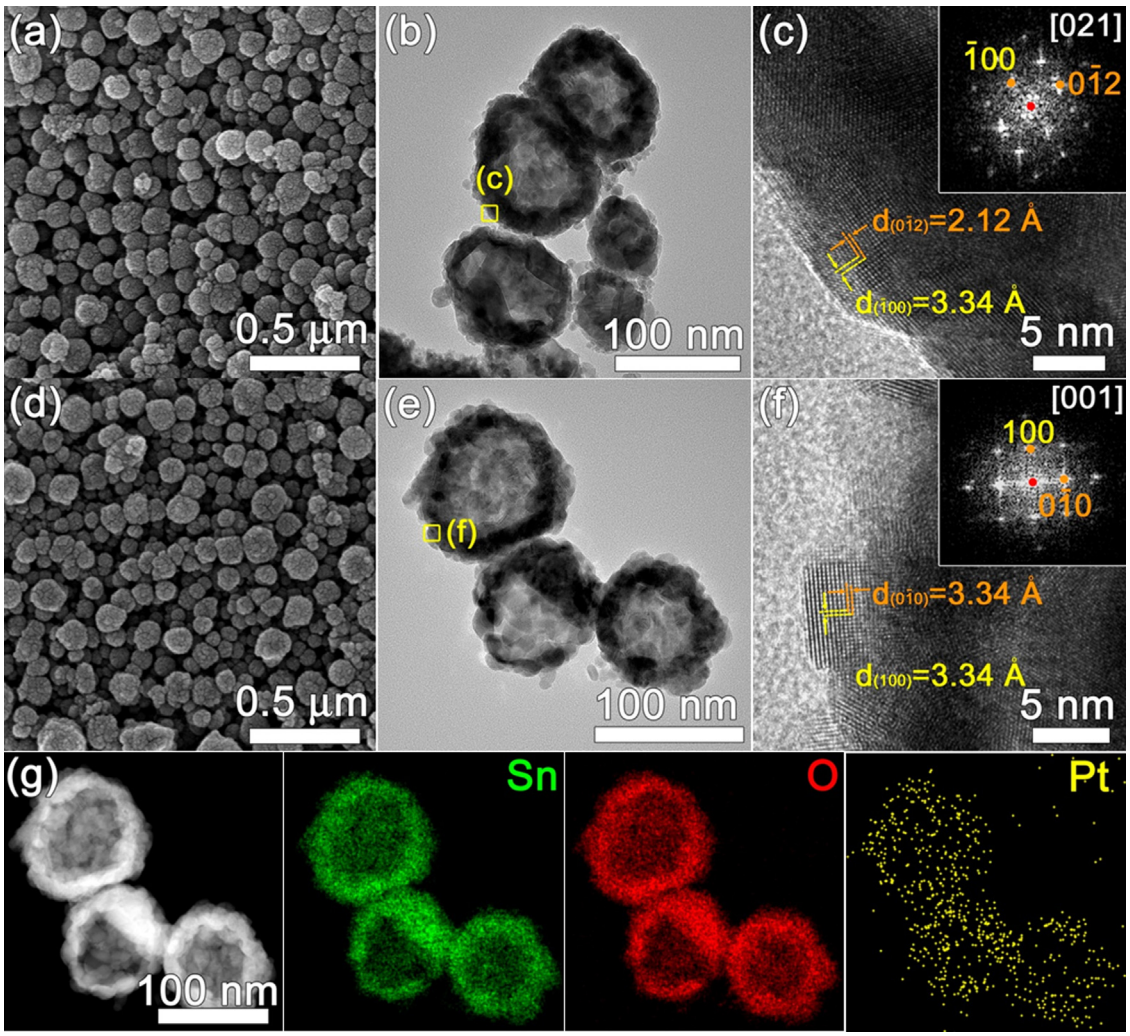

Fig. 2. SEM, TEM, and lattice-resolved TEM images, and fast Fourier transform patterns of (a–c) pure SnO_2 hollow nanospheres and (d–f) 0.3 wt% Pt-doped SnO_2 hollow nanospheres; (g) elemental mappings of 0.3 wt% Pt-doped SnO_2 hollow nanospheres for Sn, O, and Pt.

nanospheres and Pt-doped SnO_2 hollow nanospheres were similar (11.3–12.0 μm). The gas responses ($S = R_a/R_g$; R_a = resistance in air, R_g = resistance in gas) of the sensors to 5 ppm C_2H_5OH, acetone, NH_3, *p*-xylene, toluene, benzene, HCHO, CO, and H_2 were measured by switching gas atmospheres at 325–450 °C. The gas concentrations were controlled by changing the mixing ratio of the parent gases (5 ppm C_2H_5OH, acetone, NH_3, *p*-xylene, toluene, benzene, HCHO, CO, and 100 ppm H_2, all in dry synthetic air balance) and dry synthetic air. The DC two-probe resistances were measured using an electrometer interfaced with a computer.

3. Results and discussion

As-sprayed SnC_2O_4-PVP composite spheres were converted into Sn-C composite hollow spheres (Fig. 1a–c) by heat treatment at 400 °C for 3 h in a 10% H_2/Ar atmosphere. Spherical nanoparticles are observed on the surfaces of the hollow spheres in high magnification SEM (Fig. 1a, inset), which were confirmed as Sn nanocrystals in the TEM analysis (Fig. 1b) and X-ray diffraction (Fig. 1c). The Pt-doped Sn-C hollow microspheres (Fig. 1d) also contained spherical Pt-doped Sn nanocrystals (Fig. 1e and f). The uniform contours in the TEM images indicate that Sn nanocrystals in the pure and Pt-doped samples have dense inner structures and are uniformly dispersed within a carbon matrix. This results from the carbonization of PVP and crystallization of Sn-precursors during heat treatment in a reducing atmosphere. The Sn-C and Pt-doped Sn-C composite hollow spheres (Fig. 1a and d) were 25–50 μm in diameter and their shells were 0.5–1.0 μm thick, for both the pure and Pt-doped cases. Average diameters of the Sn nanocrystals embedded in the Sn-C and Pt-doped Sn-C spheres were 113 ± 40 and 109 ± 34 nm, respectively, with around 300 samples observed for each. The small size of the Sn nanocrystals and the narrow distribution can be attributed to the restrained growth of metallic Sn particles within the confined thin shells (thickness: 0.5–1.0 μm thick) of the Sn-C composite spheres. The effective separation observed between Sn nanoparticles in the carbon matrix is advantageous in the next step of preparing well-defined SnO_2 hollow nanospheres by self-templated Kirkendall diffusion process.

The pure and Pt-doped SnO_2 nanospheres were prepared by heat treatment of the Sn-C composite spheres at 500 °C in an air atmosphere for 5 h; SEM and TEM images of the products are shown in Fig. 2. Both pure and Pt-doped samples show spherical morphologies with a narrow size distribution (Fig. 2a and d). Bright contour at the centers of particles clearly shows that pure and Pt-doped SnO_2 spheres are hollow (Fig. 2b and e). Lattice-resolved TEM image and fast-Fourier transform patterns confirm that hollow spheres are highly crystalline SnO_2 (Fig. 2c and f). Elemental mapping of Sn, O, and Pt shows that the Pt component in the Pt-doped SnO_2 nanospheres is uniformly distributed (Fig. 2g). The average diameters of pure and Pt-doped SnO_2 nanospheres were

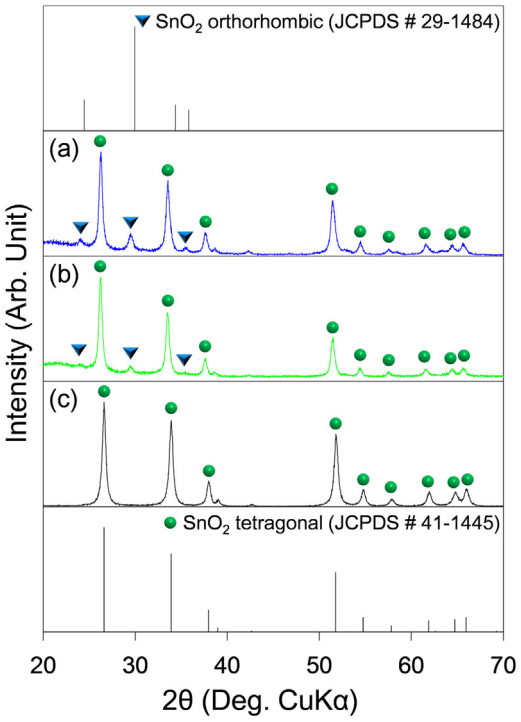

Fig. 3. X-ray diffraction patterns of (a) pure SnO_2 hollow nanospheres, (b) Pt-doped SnO_2 hollow nanospheres, and (c) commercial SnO_2 powders.

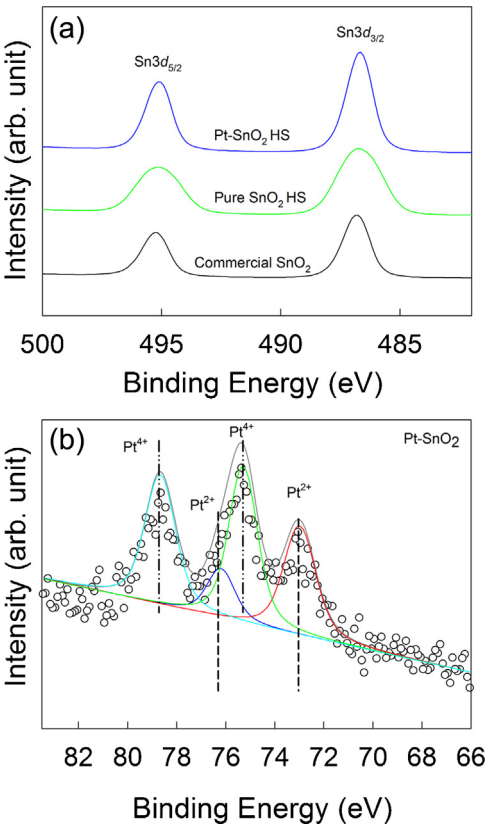

Fig. 4. X-ray photoelectron spectroscopy of (a) commercial SnO_2 powders and pure and 0.3 wt% Pt-doped SnO_2 hollow nanospheres: (a) Sn 3d and (b) Pt 4f.

calculated to be 99.2 ± 57.6 nm and 98.4 ± 68.2 nm, respectively, for samples of around 300 of each. The similar morphology and size of Sn nanocrystals and SnO_2 hollow nanospheres verifies that the SnO_2 hollow nanospheres are formed by self-templated Kirkendall diffusion during oxidation of the Sn nanospheres. The TG analyses of two different precursors (Fig. S1) confirmed the complete oxidation of carbon component and Sn metal during the heat treatment in air below 500 °C.

During heat treatment in an air atmosphere, the carbon component is oxidized into CO_2 and the metallic Sn nanospheres are oxidized from the surface. The tin oxide shell layer can grow either by the outward diffusion of Sn cations from the core metal part or by inward diffusion of oxygen from the ambient atmosphere. Two authors [18] in the present study have prepared nanofibers constituted of: Sn@void@SnO/SnO_2 yolk-shell nanospheres, SnO(inner shell)/SnO_2(outer shell) hollow nanospheres, and SnO_2 hollow nanospheres, by heat treatment of Sn-C composite nanofibers for 2 h at 400, 500, and 600 °C, respectively. Gaiduk et al. [19] also reported that solid evacuation during the oxidation of metallic Sn depends on the ambient oxygen partial pressure. These clearly suggest that the solid evacuation in the present study is also due to the Kirkendall diffusion process because of relatively rapid outward diffusion of Sn compared to inward diffusion of oxygen during the oxidation of Sn nanocrystals.

The hollow nanospheres prepared by heat treatment of Sn-C composite spheres at 500 °C in air atmosphere for 5 h were identified as tetragonal SnO_2 (JCPDS# 41-1445) containing a small amount of the orthorhombic SnO_2 phase (JCPDS# 29-1484) (Fig. 3a). No SnO phase was observed in the present study, in contrast to the previous contribution [18] in which heat treatment of Sn-C composite nanofibers at 500 °C for 2 h yielded nanofibers containing SnO/SnO_2 hollow spheres. The absence of SnO in the present study can be attributed to oxidation of the SnO phase at 500 °C during the prolonged heat treatment (5 h). The orthorhombic SnO_2 (*o*-SnO_2) phase is metastable and is known to form under high pressure [20,21]. However, the oxidation of Sn nanocrystals [22], the decomposition of SnC_2O_4 [23], and oxidation of SnO [24] are also reported to form the orthorhombic phase as a reaction intermediate; all of which involve the oxidation of metallic or divalent Sn. In all cases, the amount of orthorhombic phase decreases with increasing temperature or time in the heat treatment. In the present study, oxygen will be preferentially consumed to oxidize the carbon component in the Sn-C composite spheres and thus the full oxidation and transformation of Sn nanocrystals into the more stable tetragonal SnO_2 (*t*-SnO_2) phase may require a longer reaction time at the higher temperature. This explains the formation of the orthorhombic phase in the present study. Further, the decrease of the orthorhombic phase down to negligibly low concentration with Pt-doping (Fig. 3b) in the present study can be also explained by Pt-induced catalytic promotion of SnO oxidation and consequent transformation from *o*-SnO_2 to *t*-SnO_2 during heat treatment. The lack of a visible Pt-related peak in Fig. 3b was likely a result of the low detection limit in X-ray diffraction or of the doping of Pt into the SnO_2 lattice. From the Scherrer's equation, the crystallite sizes of pure SnO_2 hollow nanospheres, Pt-doped SnO_2 hollow nanospheres, and commercial SnO_2 powders were determined to be 33.5 ± 7.3 nm, 31.7 ± 5.5 nm, and 35.4 ± 3.5 nm, respectively.

The pure and Pt-doped SnO_2 hollow nanospheres were analyzed using XPS (Fig. 4). The Sn $3d_{5/2}$ and Sn $3d_{3/2}$ peaks are located at 495.2 eV and 486.7 eV, respectively, in pure SnO_2 hollow nanospheres (Fig. 4a), which suggests the presence of Sn^{4+} [25]. No shifts of the Sn 3*d* peaks between the pure SnO_2 and Pt-doped SnO_2 hollow nanospheres were observed. Murata et al. [26] reported a shift (0.1 eV) of the Sn 3*d* peaks to slightly lower energies for doping concentrations of Pt higher than 9 at%. The binding energy curve of Pt 4*f* in Pt-doped SnO_2 hollow spheres is deconvoluted into Pt^{2+} and Pt^{4+} in Fig. 4b. The Pt $4f_{7/2}$ peaks in Pt-doped SnO_2 hollow nanospheres are located at 73.0 eV and 75.3 eV, respectively. In

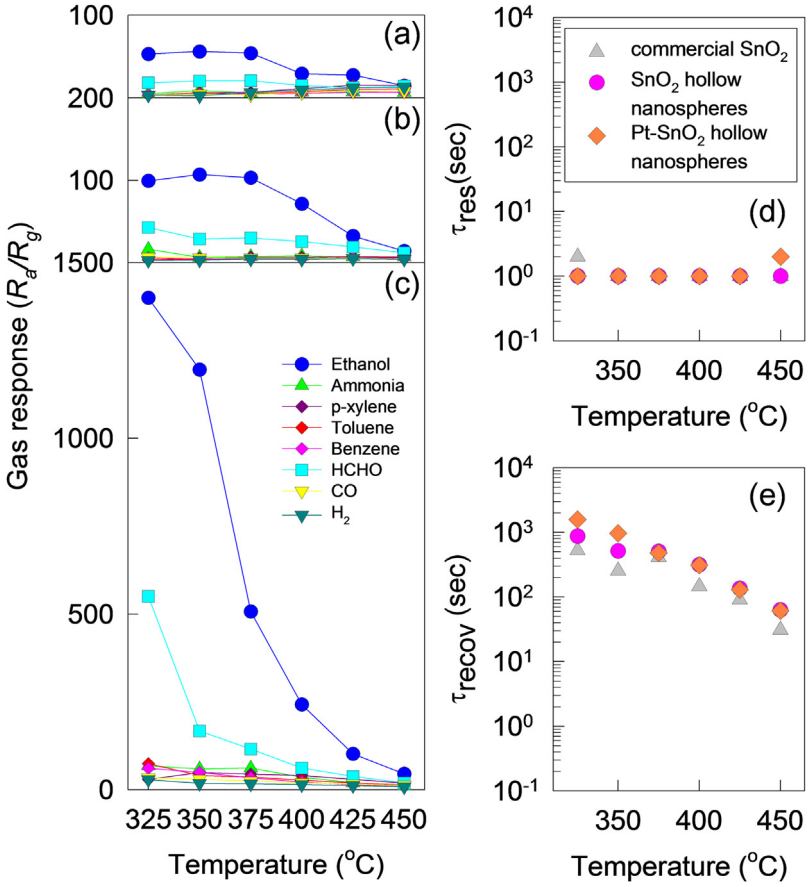

Fig. 5. Gas response (R_a/R_g) of sensors using (a) commercial SnO_2 powders, (b) pure SnO_2 hollow nanospheres, and (c) Pt-doped SnO_2 hollow spheres at 325–450 °C; (d) 90% response time (τ_{res}) and (e) 90% recovery time (τ_{recov}) of three sensors upon exposure to 5 ppm ethanol and air at 325–450 °C.

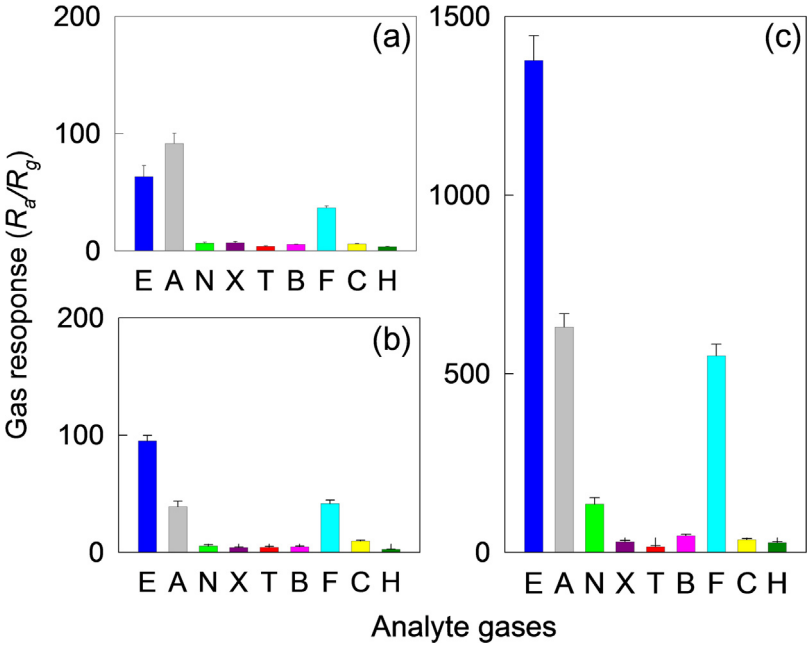

Fig. 6. Gas selectivity of (a) commercial SnO_2 powders, (b) pure SnO_2 hollow nanospheres, and (c) Pt-doped SnO_2 hollow nanospheres at 325 °C (concentration of all analyte gases: 5 ppm; E: C_2H_5OH, A: acetone, N: NH_3, X: *p*-xylene, T: toluene, B: benzene, F: HCHO, C: CO, and H: H_2). Gas sensing characteristics of 5 different sensors were measured to get the average values of gas responses.

contrast, metallic Pt peaks (70–71 eV) [27] were not detected in the Pt-doped nanospheres. The crystal structure of PtO_2 is similar to that of Cassiterite SnO_2 [28]. This suggests that the incorporation of Pt^{2+} and Pt^{4+} into the SnO_2 lattice without formation of

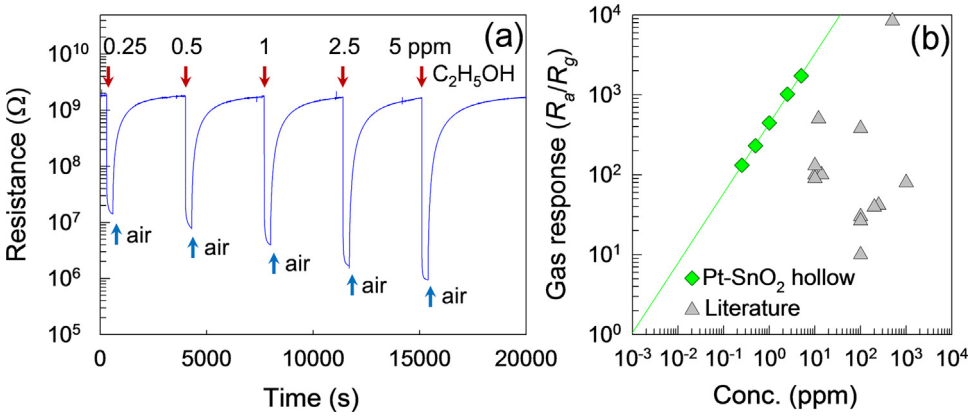

Fig. 7. (a) Sensing transients of Pt-doped SnO_2 hollow nanospheres exposed to 0.25–5 ppm C_2H_5OH at 325 °C. (b) Gas sensor response (R_a/R_g) of Pt-doped SnO_2 hollow nanospheres as a function of C_2H_5OH concentration at 325 °C (this study); C_2H_5OH sensor responses in the literature [29–41].

metallic Pt nanoclusters is probable although further systematic study is necessary to confirm this.

The gas sensing characteristics of commercial SnO_2 powders, pure, and 0.3 wt% Pt-doped SnO_2 hollow nanospheres were measured at 325–450 °C (Fig. 5). All three sensors showed their highest response to 5 ppm C_2H_5OH and second highest response to 5 ppm HCHO. However, the absolute gas responses were significantly different from each other. The sensor response (S) with SnO_2 hollow nanospheres at 325 °C was 93.3 (Fig. 5b), which is 1.8 times higher than that of commercial SnO_2 powders (S = 53.0) (Fig. 5a) at the same temperature. The response of 0.3 wt% Pt-doped SnO_2 hollow nanospheres to 5 ppm C_2H_5OH was as high as 1399.9 at 325 °C (Fig. 5c), which is 15 times higher than that of pure SnO_2 hollow spheres.

The 90% response time (τ_{res}) and 90% recovery time (τ_{recov}), the times to reach 90% variation of sensor resistance upon exposure to 5 ppm C_2H_5OH and air, were calculated from the sensing transients and the results are given in Fig. 5d and e. All 3 different sensors showed very short τ_{res} values (1–2 s), indicating that the reaction between C_2H_5OH and negatively charged oxygen on the surface occurs rapidly. In contrast, the τ_{recov} values of 3 sensors are long (525–1577 s) at 325 °C and tended to decrease to 31–61 s with increasing sensor temperature to 450 °C. Long recovery time at low sensing temperature can be attributed to the sluggish serial reactions involving the adsorption, dissociation, and ionization of oxygen on the surface and the decrease of recovery time with increasing sensing temperature can be explained by the thermal promotion of above reaction. In general, the higher gas response, the longer time is required for recovery because the more oxygen should be re-adsorbed. This explains the reason why the sensor using Pt-doped SnO_2 hollow nanospheres shows relatively longer recovery time.

The highest response and selectivity to C_2H_5OH are expected at the lower sensing temperature used, as the response to C_2H_5OH tends to decrease with sensor temperature in the range up to 450 °C. To examine gas selectivity, the responses to 5 ppm C_2H_5OH, acetone, NH_3, *p*-xylene, toluene, benzene, HCHO, CO, and H_2 at 325 °C were compared (Fig. 6a–c). In the selectivity measurement, the gas responses of 5 sensors were measured in each experimental condition to check the fluctuation of gas response and the reproducibility of sensor. The sensor using commercial SnO_2 powders showed similar responses to 5 ppm C_2H_5OH and acetone (Fig. 6a). In comparison, pure and 0.3 wt% Pt-doped SnO_2 hollow nanospheres showed the selective detection of C_2H_5OH with reduced cross-response from interfering gases (Fig. 6b and c). In particular, the sensor using Pt-doped SnO_2 nanospheres showed the highest selectivity to 5 ppm C_2H_5OH.

The sensing transients of the Pt-doped SnO_2 nanospheres to 0.25–5 ppm C_2H_5OH at 325 °C show stable and reversible sensing characteristics (Fig. 7a). The response to 0.25–5 ppm C_2H_5OH is linear with concentration, and is compared to the response of other Pt-loaded SnO_2 sensors reported in the literature (Fig. 7b) [29–41]. The Pt-doped SnO_2 sensor in this study shows an unprecedentedly high response of 132.1 to the very low concentration 250 ppb C_2H_5OH. From curve fitting, the detection limit of C_2H_5OH is calculated to be ~3 ppb, using R_a/R_g > 1.5 as the criterion for gas sensing. The responses to C_2H_5OH are among the highest in comparison to other Pt-loaded SnO_2 nanostructure sensors in the literature. The responses of 0.3 wt% Pt-doped SnO_2 hollow nanospheres to 5 ppm C_2H_5OH at 325 °C were relatively stable for 21 days, demonstrating the sensor stability (Fig. S2). This indicates that the sensor using 0.3 wt% Pt-doped SnO_2 hollow nanospheres prepared by Kirkendall diffusion in the present study offers ultrasensitive, selective, and stable detection of ppb-level C_2H_5OH, which could be used in applications such as non-invasive screening of intoxicated drivers from sweat or exhaled breath.

The significantly different gas sensing characteristics of the three sensors compared in this study, and the unprecedentedly high gas response of Pt-doped SnO_2 hollow nanospheres, should be examined with regard to the key parameters determining the response. From a Scherrer's formula analysis of the XRD patterns, crystallite sizes in the three sensor materials were similar. The BET specific surface area of commercial SnO_2 powders, SnO_2 hollow nanospheres, and Pt-doped SnO_2 hollow nanospheres were determined to be 33.6, 22.6, and 23.6 m^2/g, respectively. Note that pure SnO_2 hollow nanospheres showed a higher response to C_2H_5OH compared to commercial SnO_2 nanopowders, despite having a lower specific surface area (22.6 m^2/g compared to 33.6 m^2/g). This indicates that the gas response in the present study is mainly determined by parameters other than particle size.

Significant agglomeration between primary particles was found in the sensor fabricated using commercial SnO_2 nanopowders (Fig. S3). Considering that the van der Waals attraction is stronger for smaller particles, the formation of large agglomerates is very difficult to avoid. When this occurs, only primary particles at the outer edges of dense agglomerates will participate in gas sensing reactions, while those in the inner regions remain insensitive, leading to a relatively low gas response overall. In contrast, SnO_2 hollow nanospheres with diameters of ~100 nm in the present study show a relatively well-dispersed configuration (Fig. 2a). Thus, most of the SnO_2 hollow nanospheres can exhibit higher accessibility to analyte gas. In addition, more effective electron depletion will be obtained in hollow nanospheres because the shells' thickness (15–20 nm) is comparable to the thickness of the electron depletion layer formed

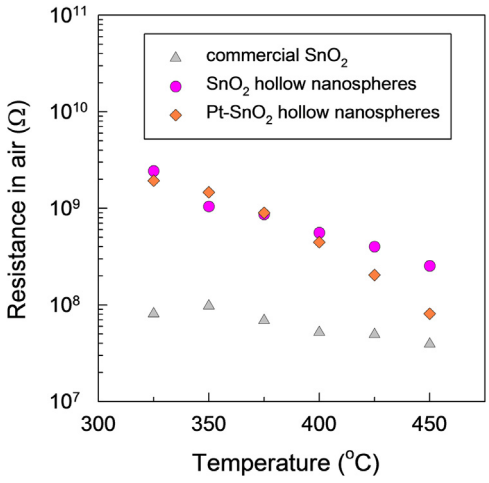

Fig. 8. Sensor resistances with commercial SnO_2 powders, pure SnO_2 hollow nanospheres, and Pt-doped SnO_2 hollow nanospheres at 325–450 °C in air atmosphere.

by oxygen adsorption. This interpretation is supported by the R_a value of sensors using pure SnO_2 hollow nanospheres being more than 1 order of magnitude higher than those of sensors using commercial SnO_2 powders at temperatures <400 °C (Fig. 8).

The effect of the minor orthorhombic phase, whose presence is noted in Fig. 3a and b, should also be discussed. Several studies have been reported but the role of the orthorhombic phase in gas sensing remains inconsistent. Ahn et al. [42] reported that a mixture of tetragonal and orthorhombic SnO_2 shows lower H_2 response compared to pure tetragonal SnO_2 powders with similar particle sizes, and suggested different oxygen adsorption on the orthorhombic phase as the reason. Hu et al. [23] prepared SnO_2 nanorods containing both t-SnO_2 and o-SnO_2 phases by calcination of SnC_2O_4, and Gu et al. [43] also prepared a mixture of t-SnO_2 and o-SnO_2 by heat treatment of SnO. In both reports, the gas response of mixed phases prepared by calcining at lower temperature was higher than that of t-SnO_2 alone from calcining at a higher temperature. However, it is still difficult to accept the positive role of the o-SnO_2 phase because the orthorhombic phase content decreases with increasing crystallite size. Gu et al. [43] also prepared another set of three SnO_2 powders with various minor o-SnO_2 contents by controlling the chemical synthesis conditions. The SnO_2 powders with the highest content of o-SnO_2 and lowest surface area showed the highest response to C_2H_5OH. This can be interpreted as a positive role of o-SnO_2. Nevertheless, considering that the responses of three SnO_2 powders with different o-SnO_2 content to 100 ppm C_2H_5OH were not significantly different from each other (S = 22.5–27.5), the positive effect of o-SnO_2 on gas sensing reactions cannot be regarded as significant. Finally, one of the present authors [44] controlled the content of the o-SnO_2 phase by changing the holding time during calcination of the SnC_2O_4 precursors at 450 °C. The response to CO increased with decreasing o-SnO_2 phase despite particle coarsening, which suggests a detrimental role of the o-SnO_2 phase. In the present study, the oxidation of Sn nanospheres will form SnO-SnO_2 core-shell hollow spheres by limited inward diffusion of oxygen, which is likely to form o-SnO_2-t-SnO_2 core-shell hollow spheres after further oxidation, based on reports that o-SnO_2 phase is formed by oxidation of SnO. This suggests that the effect of the o-SnO_2 phase on gas response may be regarded as not significant because the gas sensing reaction will occur mainly at the outer region where there is abundant t-SnO_2 phase in the hollow nanospheres. This is also supported by the observation that SnO_2 hollow nanospheres containing an o-SnO_2 phase show 1.8 times higher ethanol response compared to commercial SnO_2 powders without the o-SnO_2 phase.

In contrast, Pt catalysts play a significant role in gas sensing reactions. The noble metal catalysts can enhance gas response either by electronic or chemical sensitization. Electronic sensitization takes electrons from the n-type oxide semiconductors, extending the electron depletion layer beneath the catalyst, which increases chemiresistive variation. Chemical sensitization promotes gas sensing reactions by enhancement of the adsorption and dissociation of analyte gases. The R_a values of Pt-doped SnO_2 hollow nanospheres are similar to those of pure SnO_2 hollow nanospheres (Fig. 8), indicating that chemical rather than electronic sensitization is a more probable reason for the 15 fold increase of the ethanol response. This is supported by the report [45] that the co-existence of Pt and SnO_2 synergistically promotes the oxidation of ethanol. The above results clearly show that ultrahigh response and selectivity to ethanol in Pt-doped SnO_2 hollow nanospheres are attributable to the effective electron depletion of hollow nanospheres formed by the Kirkendall diffusion process and the promotion of gas sensing reactions by highly catalytic Pt.

4. Conclusions

Highly crystalline Pt-doped SnO_2 hollow nanospheres with a diameter of ~100 nm and shell thickness of 15–20 nm were prepared by a facile and cost-effective process that combined spray drying and nanoscale Kirkendall diffusion. This material showed ultrahigh gas sensing response and selectivity for ppm-level ethanol. The tin oxalate-PVP composite microspheres were formed by spray drying, which were converted into carbon spheres embedded with metallic Sn nanospheres by heat treatment in a reducing atmosphere. Well-defined pure and Pt-doped SnO_2 nanospheres were prepared by a self-templated Kirkendall diffusion process during the oxidation of uniformly distributed Sn nanospheres in carbon matrix. The Pt-doped SnO_2 nanospheres showed ultrahigh response (resistance ratio = 1399.9) and selectivity to 5 ppm C_2H_5OH. The unprecedentedly high gas response was attributed to the effective electron depletion of hollow spheres with thin shells and the promotion of gas sensing reactions by catalytic Pt.

Acknowledgement

This work was supported by the National Research Foundation of Korea (NRF) grant funded by the Korea Government (MEST) (No. 2013R1A2A1A01006545).

Appendix A. Supplementary data

Supplementary data associated with this article can be found, in the online version, at http://dx.doi.org/10.1016/j.snb.2016.05.002.

References

[1] N. Yamazoe, Toward innovations of gas sensor technology, Sens. Actuators B 108 (2005) 2–14.
[2] N. Barsan, N. Weimar, Conduction model of metal oxide gas sensors, J. Electroceram. 7 (2001) 143–167.
[3] M.E. Franke, T.J. Koplin, U. Simon, Metal and metal oxide nanoparticles in chemiresistors: does the nanoscale matter? Small 2 (2006) 36–50.
[4] Y. Shimizu, M. Egashira, Basic aspects and challenges of semiconductor gas sensors, MRS Bull. 24 (1999) 18–24.
[5] J.-H. Lee, Gas sensors using hierarchical and hollow oxide nanostructures: overview, Sens. Actuators B 140 (2009) 319–336.
[6] S.-J. Kim, I.-S. Hwang, C.-W. Na, I.-D. Kim, Y.C. Kang, J.-H. Lee, Ultrasensitive and selective C_2H_5OH sensors using Rh-loaded In_2O_3 hollow spheres, J. Mater. Chem. 21 (2011) 18477–18848.

[7] Y.H. Cho, Y.C. Kang, J.-H. Lee, Highly selective and sensitive detection of trimethylamine using WO_3 hollow spheres prepared by ultrasonic spray pyrolysis, Sens. Actuators B 176 (2013) 971–977.
[8] Q. Zhao, Y. Gao, X. Bai, C. Wu, Y. Xie, Facile synthesis of SnO_2 hollow nanospheres and applications in gas sensors and electrocatalysts, Eur. J. Inorg. Chem. (2006) 1643–1648.
[9] H.-J. Kim, K.-I. Choi, A. Pan, I.-D. Kim, H.-R. Kim, K.-M. Kim, C.-W. Na, G. Cao, J.-H. Lee, Template-free solvothermal synthesis of hollow hematite spheres and their applications in gas sensors and Li-ion batteries, J. Mater. Chem. 21 (2011) 6549–6555.
[10] X.-L. Li, T.-J. Lou, X.-M. Sun, Y.-D. Li, Highly sensitive WO_3 hollow-sphere gas sensors, Inorg. Chem. 43 (2004) 5442–5449.
[11] C.J. Martinez, B. Hockey, C.B. Montgomery, S. Semancik, Porous tin oxide nanostructured microspheres for sensor applications, Langmuir 21 (2005) 7937–7944.
[12] F. Gyger, M. Hübner, C. Feldmann, N. Barsan, U. Weimar, Nanoscale SnO_2 hollow spheres and their application as a gas-sensing material, Chem. Mater. 22 (2010) 4821–4827.
[13] D. Wang, J. Xu, Q. Pan, Fabrication and gas-sensing properties of hollow SnO_2 microspheres, Chem. Lett. 37 (2008) 1086–1087.
[14] Y. Yin, R.M. Rioux, C.K. Erdonmez, S. Hughes, G.A. Somorjai, A.P. Alivisators, Formation of hollow nanocrystals through the nanoscale Kirkendall effect, Science 304 (2004) 711–714.
[15] X. Song, L. Gao, S. Mathur, Synthesis, characterization, and gas sensing properties of porous nickel oxide nanotubes, J. Phys. Chem. C 115 (2011) 21730–21735.
[16] Y.-H. Choi, D.-H. Kim, H.S. Han, S. Shin, S.-H. Hong, K.S. Hong, Direct printing synthesis of self-organized copper oxide hollow spheres on a substrate using copper(II) complex ink: gas sensing and photochemical properties, Langmuir 30 (2014) 700–709.
[17] P. Wu, N. Du, H. Zhang, C. Zhai, D. Yang, Self-templating synthesis of SnO_2-carbon hybrid hollow spheres for superior lithium ion storage, ACS Appl. Mater. Interfaces 3 (2011) 1946–1952.
[18] S.J. Cho, Y.C. Kang, Nanofibers comprising yolk-shell Sn@void@SnO/SnO_2 and hollow SnO/SnO_2 and SnO_2 nanospheres via the Kirkendall diffusion effect and their electrochemical properties, Small 11 (2015) 4673–4681.
[19] P.I. Gaiduk, J.L. Hansen, A.N. Larsen, Synthesis and analysis of hollow SnO_2 nanoislands, Appl. Phys. Lett. 92 (2008) 193112.
[20] S.R. Shieh, A. Kubo, T.S. Duffy, V.B. Prakapenka, G. Shen, High-pressure phase in SnO_2 to 117 GPa, Phys. Rev. B 73 (2006) 014105.
[21] K. Suito, N. Kawai, Y. Masuda, High pressure synthesis of orthorhombic SnO_2, MRS Bull. 10 (1975) 677–680.
[22] M.-Y. Huh, S.-H. Kim, J.-P. Ahn, J.-K. Park, B.-K. Kim, Oxidation of nanophase tin particles, Nanostruct. Mater. 11 (1999) 211–220.
[23] D. Hu, B. Han, S. Deng, Z. Feng, Y. Wang, J. Popovic, M. Nuskol, Y. Wang, I. Djerdj, Novel mixed phase SnO_2 nanorods assembled with SnO_2 nanocrystals for enhancing gas-sensing performance toward isopropanol gas, J. Phys. Chem. C 118 (2014) 9832–9840.
[24] J.H. Shin, H.M. Park, J.Y. Song, Phase transformation of hierarchical nanobranch structure from SnO to SnO_2 and its electrochemical capacitance, J. Alloys Compd. 551 (2013) 451–455.
[25] L. Yan, J.S. Pan, C.K. Ong, XPS studies of room temperature magnetic Co-doped SnO_2 deposited on Si, Mater. Sci. Eng. B 128 (2006) 34–36.
[26] N. Murata, T. Suzuki, M. Kobayashi, F. Togoh, K. Asakura, Characterization of Pt-doped SnO_2 catalyst for a high performance micro gas sensor, Phys. Chem. Chem. Phys. 15 (2013) 17938–17946.
[27] N.G. Cho, G.C. Whitfield, D.J. Yang, H.-G. Kim, H.L. Tuller, I.D. Kim, Facile synthesis of Pt functionalized SnO_2 hollow hemispheres and their gas sensing properties, J. Electrochem. Soc. 157 (2010) J435–J439.
[28] L. Mädler, T. Sahm, A. Gurlo, J.-D. Grunwaldt, N. Barsan, U. Weimer, S.E. Pratsinis, Sensing low concentrations of CO using flame-spray-made Pt/SnO_2 nanoparticles, J. Nano Res. 8 (2006) 783–796.
[29] S. Moghadam, S. Zendehdell, A. Rouhollahi, Sensitivity enhancemenet in SnO_2 based gas sensors by surface decoration with platinum nanoparticles, 2014 22nd Iranian Conference on Electrical Engineering (ICEE) (2014) 341–345.
[30] E. Comini, S. Bianchi, G. Faglia, M. Ferroni, A. Vomiero, G. Sberveglieri, Functional nanowires of tin oxide, Appl. Phys. A 89 (2007) 73–76.
[31] X. Xue, Z. Chen, C. Ma, L. Xing, Y. Chen, Y. Wang, T. Wang, One-step synthesis and gas-sensing characteristics of uniformly loaded Pt@SnO_2 nanorods, J. Phys. Chem. C 114 (2010) 3968–3972.
[32] X. Liu, N. Chen, B. Han, X. Xiao, G. Chen, I. Djerdj, Y. Wang, Nanoparticle cluster gas sensor: Pt activated SnO_2 nanoparticles for NH_3 detection with ultrahigh sensitivity, Nanoscale 7 (2015) 14872–14880.
[33] X.Y. Xue, Z.H. Chen, Y.J. Chen, C.H. Ma, L.L. Xing, Y.G. Wang, T.H. Wang, Abnormal gas sensing characteristics arising from catalyzed morphological changes of ionsorbed oxygen, Nanotechnology 21 (2010) 065501.
[34] Y.H. Lin, Y.C. Hsueh, P.S. Lee, C.C. Wang, J.M. Wu, T.P. Perng, H.C. Shih, Fabrication of tin dioxide nanowires with ultrahigh gas sensitivity by atomic layer deposition of platinum, J. Mater. Chem. 21 (2011) 10552–10558.
[35] G. Neri, A. Bonavita, G. Micali, N. Donato, F.A. Deorsola, P. Mossino, I. Amato, B. De Benedetti, Ethanol sensors based on Pt-doped tin oxide nanopowders synthesized by gel-combustion, Sens. Actuators B 117 (2006) 196–204.
[36] P. Ivanov, E. Llobet, X. Vilanova, J. Brezmes, J. Hubalek, X. Correig, Development of high sensitivity ethanol gas sensors based on Pt-doped SnO_2 surfaces, Sens. Actuators B 99 (2004) 201–206.
[37] K.Y. Dong, J.K. Choi, I.S. Hwang, J.W. Lee, B.H. Kang, D.J. Ham, B.K. Ju, Enhanced H_2S sensing characteristics of Pt doped SnO_2 nanofibers sensors with micro heater, Sens. Actuators B 157 (2011) 154–161.
[38] Y.H. Lin, Y.C. Hsueh, P.S. Lee, C.C. Wang, J.R. Chen, J.M. Wu, T.-P. Perng, H.C. Shih, Preparation of Pt/SnO_2 core–shell nanowires with enhanced ethanol gas- and photon-sensing properties, J. Electrochem. Soc. 157 (2010) K206–K210.
[39] S.N. Oliaee, A. Khodadadi, Y. Mortazavi, S. Alipour, Highly selective Pt/SnO_2 sensor to propane or methane in presence of CO and ethanol, using gold nanoparticles on Fe_2O_3 catalytic filter, Sens. Actuators B 147 (2010) 400–405.
[40] P. Lv, Z. Tang, G. Wei, J. Yu, Z. Huang, Recognizing indoor formaldehyde in binary gas mixtures with a micro gas sensor array and a neural network, Meas. Sci. Technol. 18 (2007) 2997.
[41] C. Bittencourt, E. Llobet, P. Ivanov, X. Correig, X. Vilanova, J. Brezmes, J. Hubalek, K. Malysz, J.J. Pireaux, J. Calderer, Influence of the doping method on the sensitivity of Pt-doped screen-printed SnO_2 sensors, Sens. Actuators B 97 (2004) 67–73.
[42] J.P. Ahn, S.-H. Kim, J.-K. Park, M.-Y. Huh, Effect of orthorhombic phase on hydrogen gas sensing property of thick-film sensors fabricated by nanophase tin dioxide, Sens. Actuators B 94 (2003) 125–131.
[43] C.D. Gu, H. Zheng, X.L. Wang, J.P. Tu, Superior ethanol-sensing behavior based on SnO_2 mesocrystals incorporating orthorhombic and tetragonal phases, RSC Adv. 5 (2015) 9143–9153.
[44] K.-W. Kim, P.-S. Cho, J.-H. Lee, S.-H. Hong, Gas sensing characteristics of SnO_2 whiskers prepared from SnC_2O_4, Rare Met. Mater. Eng. 35 (2006) 100–103.
[45] A. Kowal, S.Lj. Gojković, P. Lee, Y.-E. Sung, Synthesis, characterization and electrocatalytic activity for ethanol oxidation of carbon supported Pt, Pt-Rh, Pt-SnO_2 and Pt-Rh-SnO_2 nanoclusters, Electrochem. Commun. 11 (2009) 724–727.

Biographies

Bo-Young Kim studied Materials Science and Engineering and received his BS degree in 2014 from Seoul National University of Science and Technology. She is currently studying for an M.S./Ph.D. integrated degree at Korea University. Her research interest is oxide semiconductor gas sensors using nanostructures.

Jung Sang Cho studied Chemical Engineering and received his B.S. from Konkuk University, Korea, in 2006. He is currently post-doctoral researcher at Korea University. His research interests are nanostructured materials for Li-ion batteries.

Ji-Wook Yoon studied Materials Science and Engineering and received his B.S. from Korea University, Korea, in 2011. He is currently studying for an M.S./Ph.D. integrated degree at Korea University. His research interests are gas sensors using oxide nanofibers and yolk-shell nanostructures.

Chan Woong Na received his BS, MS, and PhD degrees from Korea University in 2004, 2006, and 2012, respectively. He was researcher at OCI Corporation (2006–2009), senior researcher at Samsung SDI (2012–2015), Since 2015, he has been a research professor at Korea University, Seoul, Korea. His research interests are nanostructure-based gas sensors and energy applications.

Chul-Soon Lee studied materials science and engineering and received his MS degree in 2013, from Korea University. He is currently a Ph.D. student at Korea University. His research topic is gas sensors using porous metal oxide thin films.

Jee Hyun Ahn studied Materials Science and Engineering and received his B.S. from Korea University, Korea, in 2011. She is currently studying for an M.S./Ph.D. integrated degree at Korea University. Her research interests are SOFC electrolytes and Li-ion batteries.

Yun Chan Kang joined the Department of Materials Science and Engineering at Korea University as a full professor in 2014. He received his M.S. and Ph.D. degrees from the Korea Advanced Institute of Science and Technology in 1995 and 1997, respectively. Between 2000 and 2004, he developed phosphor materials at the Korea Research Institute of Chemical Technology. He was assistant professor and associate professor at Konkuk University from 2004 to 2014. His current research interests include materials for flat panel displays, batteries, and solar cells.

Jong-Heun Lee joined the Department of Materials Science and Engineering at Korea University as an associate professor in 2003, where he is currently professor. He received his BS, MS, and Ph.D. degrees from Seoul National University in 1987, 1989, and 1993, respectively. Between 1993 and 1999, he developed automotive air-fuel-ratio sensors at the Samsung Advanced Institute of Technology. He was a Science and Technology Agency of Japan (STA) fellow at the National Institute for Research in Inorganic Materials (currently NIMS, Japan) from 1999 to 2000 and a research professor at Seoul National University from 2000 to 2003. His current research interests include chemical sensors, functional nanostructures, and solid oxide electrolytes.